Available online at www.sciencedirect.com
SCIENCE DIRECT®
Journal of Solid State Chemistry 177 (2004) 2867–2874
JOURNAL OF SOLID STATE CHEMISTRY
http://elsevier.com/locate/jssc

# $Eu_7Ga_6Sb_8$: A Zintl phase with Ga–Ga bonds and polymeric gallium antimonide chains

Seon-Mi Park,[a] Sung-Jin Kim,[a,*] and Mercouri G. Kanatzidis[b,*]

[a] *Department of Chemistry, Ewha Womans University, Seoul #120-750, South Korea*
[b] *Department of Chemistry and Center for Fundamental Materials Research, Michigan State University, 320 Chemistry Bldg, East Lansing, MI 48824, USA*

Received 20 February 2004; received in revised form 15 April 2004; accepted 16 April 2004

**Abstract**

The Zintl phase $Eu_7Ga_6Sb_8$ was obtained from a direct element combination reaction at 900°C. It crystallizes in the orthorhombic space group *Pbca* (No. 61) with $a = 15.6470(17)$ Å, $b = 17.2876(19)$ Å, $c = 17.9200(19)$ Å, and $Z = 8$. In $Eu_7Ga_6Sb_8$, the anionic framework forms infinite chains of $[Ga_6Sb_8]^{14-}$ which are arranged side by side to make a sheet-like arrangement but without linking. The sheets of chains are separated by $Eu^{2+}$ atoms and also within the sheet, $Eu^{2+}$ atoms fill the spaces between two chains. The chain is made up of homoatomic tetramers $(Ga_4)^{6+}$ and dimers $(Ga_2)^{4+}$ connected by Sb atoms. The compound is a narrow band-gap semiconductor with $E_g \sim 0.6$ eV and satisfies the classical Zintl concept. Extended Hückel band structure calculations confirm that the material is a semiconductor and suggest that the structure is stabilized by strong Ga–Ga covalent bonding interactions. Magnetic susceptibility measurements for $Eu_7Ga_6Sb_8$ show that the Eu atoms are divalent and the compound has an antiferromagnetic transition at 9 K.


## 1. Introduction

Zintl phases are compounds formed typically between very electropositive elements such as alkali or alkaline metals and electronegative main group metals such as group 14–16 metals. Zintl phases build valence-precise zero-, one-, two- or three-dimensional polyatomic frameworks [1]. These phases are of continuing interest because of the striking variety of structures. We have been interested in environmentally stable Zintl phases with complex anionic frameworks composed of heavier elements designed to be narrow-gap semiconductors because they may display useful electronic properties. To achieve stability in the ambient, we chose alkaline earth and divalent rare earth elements in conjunction with group 12, 13 elements and electronegative group 15 elements. The cations of these elements interact strongly with the electronegative main group metal framework and resist attack by outside agents such as water. This approach led to the largely air-stable Zintl anisotropic frameworks in the ternary phases $Yb_9Zn_4Pn_9$ ($Pn$ = Sb, Bi) [2], $Ba_8In_4Sb_{16}$ [3], $RE_5In_2Sb_6$ ($RE$ = Yb, Eu) [4], $BaGa_2Sb_2$ [5], and $Ba_3Ga_4Sb_5$ [6]. Related compounds such as $A_{14}TrPn_{11}$ ($A$ = Ca, Sr, Ba, Eu, Yb; $Tr$ = Al, Ga, Zn, Cd; $Pn$ = P, As, Sb, Bi) have been reported by other groups [7]. The gallium antimonides draw our attention because of their unusual ethane like "$Ga_2Sb_6$" unit found in $BaGa_2Sb_2$ [5] and $Ba_3Ga_4Sb_5$ [6]. Recently, rare earth gallium antimonides with novel homoatomic clusters such as puckered $Ga_6$-rings and $Ga_2$-pairs were reported in $La_{13}Ga_8Sb_{21}$ and $RE_{12}Ga_4Sb_{23}$ ($RE$ = La–Nd, Sm), respectively [8].

Our attempts to prepare new Zintl frameworks with group 13 elements resulted in the discovery of $Eu_7Ga_6Sb_8$, a material with a unique framework and extensive Ga–Ga bonding. We describe the synthesis, crystal structure, spectroscopic characterization, magnetic properties and electronic structure of this compound.

*Corresponding author. Fax: +517-353-1793.
*E-mail addresses:* sjkim@ewha.ac.kr (S.-J. Kim), kanatzid@cem.msu.edu (M.G. Kanatzidis).

0022-4596/$ - see front matter © 2004 Elsevier Inc. All rights reserved.
doi:10.1016/j.jssc.2004.04.025

## 2. Experimental section

### 2.1. Synthesis

The crystal used in the structure determination resulted from the reaction of a mixture of three elements (Eu, Aldrich, chip, 99%; Ga, Aldrich, chip, 99.99%; Sb, High Purity Chemicals, powder, 99.9%) in a molar ratio of 3:2:4. The reaction mixture was placed in a graphite tube and sealed in an evacuated silica tube. The mixture was then heated slowly up to 900°C for 2 d, and kept at that temperature for 1 d, and subsequently cooled to room temperature over 1 d. The reaction gave a few rod-shaped black crystals along with gray featureless pieces. Semiquantitative microprobe analysis on the single crystals gave $Eu_{7.0(2)}Ga_{5.8(2)}Sb_{8.3(2)}$ (average of three data acquisitions) and analysis on gray featureless pieces gave an unknown binary Eu–Sb phase with about Eu:Sb = 3:2 ratio. Stoichiometric reactions at the composition $Eu_7Ga_6Sb_8$ led to the formation of the product with the same minor unknown phase. The powder pattern of isolated rod-shaped black crystals agreed well with the powder pattern calculated from the single-crystal parameters. Therefore, the single crystals isolated from bulk product were used for IR, thermal and magnetic measurements.

### 2.2. Electron microscopy

Semiquantitative microprobe analysis of the compounds was performed with a JEOL JSM-35C scanning electron microscope (SEM) equipped with a Tracor Northern Energy Dispersive Spectroscopy (EDS) detector. Data were acquired using an accelerating voltage of 20 kV and a 30 s accumulation time.

### 2.3. Differential thermal analysis

Differential thermal analysis (DTA) was performed with a Shimadzu DTA-50 thermal analyzer. The ground sample (≈30.0 mg total mass) was sealed in a carbon coated silica ampoule under vacuum. A silica ampoule containing alumina of equal mass was sealed and placed on the reference side of the detector. The sample was heated to 950°C at 10°C/min and isothermed for 10 min, followed by cooling at −10°C/min to 50°C. The stability of the phase and reproducibility of the melting point of the sample were monitored by running multiple heating and cooling cycles. The residue of the DTA experiment was examined with X-ray powder diffraction. The compound $Eu_7Ga_6Sb_8$ is stable at room temperature in air, however, when the air-exposed sample is heated at about 670°C, it slowly decomposes to Ga and unknown phases. The compound melts at 670°C.

Table 1
Selected data from the single-crystal structure refinement of $Eu_7Ga_6Sb_8$

| Empirical formula | $Eu_7Ga_6Sb_8$ |
|---|---|
| Formula weight | 2456.04 |
| Temperature ($K$) | 173.1(2) |
| Wavelength ($\lambda$ = Mo$K\alpha$, Å) | 0.71073 |
| Space group | *Pbca* (No. 61) |
| Unit cell dimensions (Å) | $a = 15.6470(17)$ |
| | $b = 17.2876(19)$ |
| | $c = 17.9200(19)$ |
| Volume (Å$^3$) | 4847.3(9) |
| $Z$ | 8 |
| Density (g/cm$^3$) | 6.731 |
| Absorption coefficient (mm$^{-1}$) | 33.067 |
| Reflections collected/unique | 28133/5345 [$R$(int) = 0.0808] |
| Data/constraints/parameters | 5345/0/191 |
| Final $R$ indices [$F_o^2 > 2\sigma(F_o^2)$][a] | $R_1 = 0.0415$, w$R_2 = 0.1043$ |
| $R$ indices ($F_o^2 > 0$) | $R_1 = 0.1177$, w$R_2 = 0.1212$ |
| Largest diff. peak and hole (Å$^3$) | 2.790 and −3.046 |

With room temperature data, a smaller unit cell with parameters of $a = 9.0053(18)$ Å, $b = 15.635(3)$ Å, $c = 17.310(4)$ Å was obtained and the Laue symmetry and systematic extinctions were indicative of the higher space group *Cmcm*. The results of refinement show disordered anionic clusters with short Ga–Ga contacts at 1.279(4) and 1.541(5) Å. Obviously this is a subcell. The correct unit cell could be clearly resolved with the low temperature data set.

[a] $R_1 = [\Sigma|F_o| - |F_c|]/\Sigma|F_o|$, $wR_2 = \{[\Sigma w[(F_o)^2 - (F_C)^2]^2]/[\Sigma w(F_o^2)^2]\}^{1/2}$ for $F_o^2 > 2\sigma(F_o^2)$, $w = [\sigma^2(F_o)^2 + (0.0390P)]^{-1}$, where $P = (F_o^2 + 2F_C^2)/3$

Table 2
Atomic coordinates ($\times 10^4$) and equivalent isotropic displacement parameters (Å$^2 \times 10^3$) for $Eu_7Ga_6Sb_8$

| Atom | Wyckoff positions | $x$ | $y$ | $z$ | $U$(eq) |
|---|---|---|---|---|---|
| Eu(1) | 8$c$ | 5008(1) | 2433(1) | 6257(1) | 7(1) |
| Eu(2) | 8$c$ | 5007(1) | 30(1) | 8732(1) | 6(1) |
| Eu(3) | 8$c$ | 2539(1) | 23(1) | 7536(1) | 6(1) |
| Eu(4) | 8$c$ | 4910(1) | 38(1) | 3773(1) | 7(1) |
| Eu(5) | 8$c$ | 2500(1) | 36(1) | 4978(1) | 7(1) |
| Eu(6) | 8$c$ | 2478(1) | 2515(1) | 2480(1) | 6(1) |
| Eu(7) | 8$c$ | 2511(1) | 2510(1) | 5028(1) | 6(1) |
| Sb(1) | 8$c$ | 4189(1) | 1196(1) | 7451(1) | 6(1) |
| Sb(2) | 8$c$ | 4125(1) | 3847(1) | 5070(1) | 6(1) |
| Sb(3) | 8$c$ | 4136(1) | 1247(1) | 5047(1) | 6(1) |
| Sb(4) | 8$c$ | 4084(1) | 3786(1) | 7460(1) | 6(1) |
| Sb(5) | 8$c$ | 6678(1) | 1164(1) | 3752(1) | 6(1) |
| Sb(6) | 8$c$ | 6635(1) | 3753(1) | 6241(1) | 6(1) |
| Sb(7) | 8$c$ | 6686(1) | 1213(1) | 8734(1) | 6(1) |
| Sb(8) | 8$c$ | 6728(1) | 1228(1) | 6234(1) | 6(1) |
| Ga(1) | 8$c$ | 3435(1) | 1548(1) | 8752(1) | 7(1) |
| Ga(2) | 8$c$ | 4023(1) | 2061(1) | 3723(1) | 10(1) |
| Ga(3) | 8$c$ | 5421(1) | 2090(1) | 8109(1) | 9(1) |
| Ga(4) | 8$c$ | 5505(1) | 2018(1) | 4470(1) | 13(1) |
| Ga(5) | 8$c$ | 5745(1) | 3409(1) | 4924(1) | 10(1) |
| Ga(6) | 8$c$ | 5749(1) | 3433(1) | 7555(1) | 7(1) |

$U$(eq) is defined as one-third of the trace of the orthogonalized $U_{ij}$ tensor.

Table 3
Selected bond distances (Å) and angles (deg) in $Eu_7Ga_6Sb_8$

| | | | | | |
|---|---|---|---|---|---|
| Sb(1)–Ga(1) | 2.683(3) | Ga(1)–Ga(2) | 2.576(3) | Ga(4)–Ga(3) | 2.889(3) |
| Sb(1)–Ga(3) | 2.737(3) | Ga(1)–Sb(2) | 2.684(3) | Ga(4)–Ga(2) | 2.678(3) |
| Sb(2)–Ga(5) | 2.659(3) | Ga(1)–Sb(8) | 2.728(2) | Ga(4)–Sb(5) | 2.683(3) |
| Sb(2)–Ga(1) | 2.684(3) | Ga(1)–Sb(1) | 2.683(3) | Ga(4)–Sb(3) | 2.727(3) |
| Sb(3)–Ga(4) | 2.727(3) | Ga(2)–Ga(1) | 2.576(3) | Ga(5)–Sb(7) | 2.672(3) |
| Sb(3)–Ga(2) | 2.764(3) | Ga(2)–Ga(4) | 2.678(3) | Ga(5)–Ga(4) | 2.567(3) |
| Sb(4)–Ga(2) | 2.698(3) | Ga(2)–Sb(3) | 2.764(3) | Ga(5)–Sb(2) | 2.659(3) |
| Sb(4)–Ga(6) | 2.681(3) | Ga(2)–Sb(4) | 2.698(3) | Ga(5)–Sb(6) | 2.805(3) |
| Sb(5)–Ga(4) | 2.683(3) | Ga(2)–Ga(3) | 2.856(3) | Ga(6)–Sb(5) | 2.685(3) |
| Sb(5)–Ga(6) | 2.685(3) | Ga(3)–Ga(6) | 2.577(3) | Ga(6)–Ga(3) | 2.577(3) |
| Sb(6)–Ga(6) | 2.788(3) | Ga(3)–Ga(2) | 2.856(3) | Ga(6)–Sb(4) | 2.681(3) |
| Sb(6)–Ga(5) | 2.805(3) | Ga(3)–Ga(4) | 2.889(3) | Ga(6)–Sb(6) | 2.788(3) |
| Sb(7)–Ga(5) | 2.672(3) | Ga(3)–Sb(7) | 2.734(3) | | |
| Sb(7)–Ga(3) | 2.734(2) | Ga(3)–Sb(1) | 2.737(3) | | |
| Sb(8)–Ga(1) | 2.728(2) | Ga(4)–Ga(5) | 2.567(3) | | |
| | | | | | |
| Eu(1)–Sb(3) | 3.281(2) | Eu(3)–Sb(4) | 3.3233(19) | Eu(5)–Sb(7) | 3.330(2) |
| Eu(1)–Sb(1) | 3.285(2) | Eu(3)–Sb(5) | 3.323(2) | Eu(5)–Sb(5) | 3.336(2) |
| Eu(1)–Sb(8) | 3.4031(14) | Eu(3)–Sb(7) | 3.3443(19) | Eu(6)–Sb(7) | 3.339(2) |
| Eu(1)–Sb(6) | 3.4190(14) | Eu(3)–Sb(6) | 3.3615(19) | Eu(6)–Sb(4) | 3.361(2) |
| Eu(1)–Sb(4) | 3.494(2) | Eu(4)–Sb(3) | 3.324(2) | Eu(6)-Sb(8) | 3.384(2) |
| Eu(1)–Sb(2) | 3.522(2) | Eu(4)–Sb(4) | 3.368(2) | Eu(6)–Sb(6) | 3.440(2) |
| Eu(2)–Sb(2) | 3.262(2) | Eu(4)–Sb(1) | 3.369(2) | Eu(6)–Sb(5) | 3.455(2) |
| Eu(2)–Sb(1) | 3.312(2) | Eu(4)–Sb(8) | 3.3701(14) | Eu(6)–Sb(1) | 3.473(2) |
| Eu(2)–Sb(7) | 3.3287(14) | Eu(4)–Sb(5) | 3.3825(14) | Eu(7)–Sb(3) | 3.351(2) |
| Eu(2)-Sb(4) | 3.348(2) | Eu(4)–Sb(3) | 3.411(2) | Eu(7)–Sb(8) | 3.373(2) |
| Eu(2)–Sb(2) | 3.381(2) | Eu(5)–Sb(2) | 3.273(2) | Eu(7)–Sb(7) | 3.408(2) |
| Eu(2)–Sb(6) | 3.3888(14) | Eu(5)–Sb(8) | 3.308(2) | Eu(7)–Sb(2) | 3.424(2) |
| Eu(3)–Sb(1) | 3.2861(19) | Eu(5)–Sb(3) | 3.309(2) | Eu(7)–Sb(5) | 3.426(2) |
| Eu(3)–Sb(8) | 3.287(2) | Eu(5)–Sb(6) | 3.315(2) | Eu(7)–Sb(6) | 3.437(2) |
| | | | | | |
| Eu(1)–Ga(6) | 3.121(3) | Ga(2)–Ga(1)–Sb(1) | 92.14(9) | Ga(2)–Ga(4)–Sb(5) | 111.61(9) |
| Eu(1)–Ga(5) | 3.144(3) | Ga(2)–Ga(1)–Sb(2) | 96.42(9) | Ga(5)–Ga(4)–Sb(3) | 116.92(10) |
| Eu(1)–Ga(4) | 3.373(3) | Sb(1)–Ga(1)–Sb(2) | 122.03(8) | Ga(2)–Ga(4)–Sb(3) | 61.49(7) |
| Eu(1)–Ga(3) | 3.432(3) | Ga(2)–Ga(1)–Sb(8) | 122.63(8) | Sb(5)–Ga(4)–Sb(3) | 116.76(10) |
| Eu(2)–Ga(1) | 3.597(2) | Sb(1)–Ga(1)–Sb(8) | 113.09(9) | Ga(4)–Ga(5)–Sb(2) | 99.10(10) |
| Eu(2)–Ga(5) | 3.630(3) | Sb(2)–Ga(1)–Sb(8) | 109.51(9) | Ga(4)–Ga(5)–Sb(7) | 93.29(9) |
| Eu(3)–Ga(1) | 3.697(2) | Ga(1)–Ga(2)–Sb(4) | 122.43(11) | Sb(2)–Ga(5)–Sb(7) | 122.33(9) |
| Eu(4)–Ga(6) | 3.671(2) | Ga(4)–Ga(2)–Sb(4) | 111.92(8) | Ga(4)–Ga(5)–Sb(6) | 122.56(10) |
| Eu(4)–Ga(4) | 3.760(3) | Ga(1)–Ga(2)–Sb(3) | 118.73(10) | Sb(2)–Ga(5)–Sb(6) | 109.26(8) |
| Eu(6)–Ga(1) | 3.166(2) | Ga(4)–Ga(2)—Sb(3) | 60.12(7) | Sb(7)–Ga(5)–Sb(6) | 110.24(9) |
| Eu(6)–Ga(6) | 3.176(2) | Sb(4)–Ga(2)–Sb(3) | 116.25(8) | Ga(3)—Ga(6)–Sb(4) | 92.08(9) |
| Eu(6)–Ga(2) | 3.369(2) | Ga(6)–Ga(3)–Sb(7) | 120.90(9) | Ga(3)–Ga(6)–Sb(5) | 91.94(8) |
| Eu(6)–Ga(3) | 3.469(3) | Ga(6)–Ga(3)–Sb(1) | 118.87(9) | Sb(4)–Ga(6)–Sb(5) | 121.19(9) |
| Eu(7)–Ga(1) | 3.157(2) | Sb(7)–Ga(3)–Sb(1) | 111.93(9) | Ga(3)–Ga(6)–Sb(6) | 127.10(10) |
| Eu(7)–Ga(5) | 3.188(3) | Ga(5)–Ga(4)–Ga(2) | 105.03(11) | Sb(4)–Ga(6)–Sb(6) | 112.62(8) |
| Eu(7)–Ga(4) | 3.366(3) | Ga(5)–Ga(4)—Sb(5) | 124.56(10) | Sb(5)–Ga(6)–Sb(6) | 110.73(9) |
| Eu(7)–Ga(2) | 3.415(2) | | | | |

### 2.4. Infrared spectroscopy

Infrared diffuse reflectance spectra of $Eu_7Ga_6Sb_8$ were recorded to determine the presence of a band-gap. The sample was ground into a powder prior to the data acquisition. The spectra were recorded in mid-IR region (4000–400 $cm^{-1}$, 4 $cm^{-1}$ resolution) with a Nicolet 740 FT-IR spectrometer equipped with a diffused reflectance attachment. Absorbance values were calculated from the reflectance data using the Kubelka-Munk function [9,10]. The band-gap $E_g$ extracted from the $(\alpha/S)$ vs. energy plot was observed at $\sim$0.6 eV ($\alpha$ = absorption coefficient, $S$ = scattering constant).

### 2.5. Magnetic susceptibility measurements

Measurements for $Eu_7Ga_6Sb_8$ single crystals were performed with a MPMS Quantum Design SQUID magnetometer. A linear field dependence of the magnetization was observed. The measurements were done under increasing temperature (3 $\sim$–300 K) with a 500-G applied field.

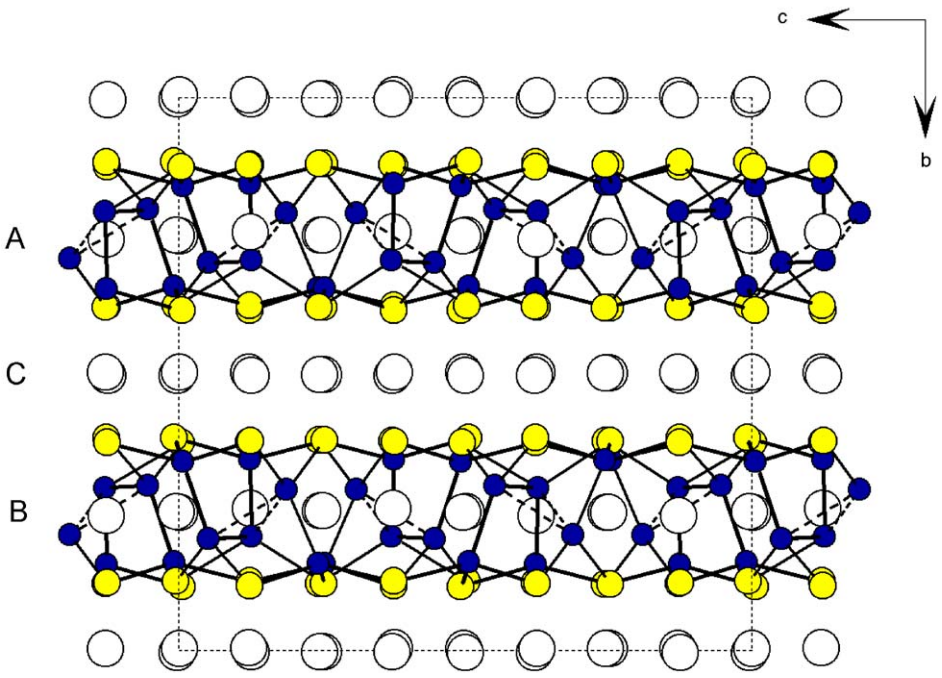


Fig. 1. A [100] view of the orthorhombic unit cell of $Eu_7Ga_6Sb_8$. The $[Ga_6Sb_8]^{14-}$ chains are not discernible in this view. The second nearest Ga–Ga distances are indicated as dotted lines. The Sb, Ga, and Eu atoms are indicated yellow, blue, and empty circles, respectively.

### 2.6. Electronic structure calculations

Electronic structure calculations were performed by the extended Hückel method within the framework of the tight-binding approximation [11]. The atomic orbital parameters employed in the calculations were default values in the CAESAR program [12,13]. Density of states (DOS) and crystal orbital overlap populations (COOP) were calculated based on 216 K point sets based on the primitive orthorhombic structure.

### 2.7. Crystallographic studies

Intensity data were collected at two different temperatures using the same black rod-shaped crystal ($0.005 \times 0.003 \times 0.01\,mm^3$) mounted glass fiber. Of course many crystals we screened before we selected one that gave reasonable diffraction properties. A Bruker AXS SMART Platform CCD diffractometer equipped with low temperature apparatus was used to collect intensity data using graphite monochromatized Mo$K_\alpha$ radiation. The one data set was collected over a half sphere of reciprocal space up to 56° in $2\theta$ at room temperature and the other data set was collected at 173.1(2) K and other procedures for data collection were similar in the two data sets. The individual frames were measured with a $\omega$ rotation of 0.3° and an acquisition time 45 s. To check the stability of the crystal, at the end of data collection procedure, the initial 50 frames of data were measured again and compared. No crystal decay was detected. The SMART software was used for data acquisition and SAINT for data extraction and reduction [14]. The absorption correction was performed empirically using SADABS [15]. With the low temperature data, the unit cell parameters were obtained from least-squares refinement using 600 randomly chosen reflections from a full sphere of reciprocal space up to 56° in $2\theta$, see Table 1. The observed Laue symmetry and systematic extinctions were indicative of the space group *Pbca* for the 173.1(2) K data set. The initial positions of all atoms were obtained with direct methods of the SHELXS-97 program. The structure was refined by full-matrix least-squares techniques with the use of the SHELXL-97 program package of crystallographic programs [16]. Once all atoms were located, the occupancies of successive atoms were allowed to vary, but refinements did not lead to any significant change in the occupation factor. For low temperature data, the final cycle of refinement performed on $F_o^2$ with 191 variables and 5345 averaged reflections converged to residuals w$R_2$ $(F_o^2 > 0) = 0.1212$. The conventional $R$ index based on reflections having $F_o^2 > 2\sigma(F_o^2)$ was 0.0415. The final difference Fourier synthesis map showed maximum and minimum peaks of 2.790 and $-3.046\,e/Å^3$, respectively. For room temperature data, the final cycle of refinement performed on $F_o^2$ with 76 variables and 1477 averaged reflections converged to residuals w$R_2$ $(F_o^2 > 0) = 0.0786$. The conventional $R$ index based on reflections having $F_o^2 > 2\sigma(F_o^2)$ was 0.0271. The final difference Fourier synthesis map showed maximum and minimum peaks of 1.149 and $-1.616\,e/Å^3$, respectively. The complete data collection

parameters and details of structure solution and refinement result are given in Table 1. Final atomic positions, equivalent isotropic displacement parameters, and selected bond distances are given in Tables 2 and 3.

## 3. Results and discussion

### 3.1. Structure

$Eu_7Ga_6Sb_8$ adopts a new structure type with infinite chains of $[Ga_6Sb_8]^{14-}$ held together with extensive Ga–Ga bonding. The chains are arranged side by side in a row along the *a*-direction forming anionic slabs parallel to the *ac*-plane. There are no inter-chain bonding interactions. The overall structure of $Eu_7Ga_6Sb_8$ is made up of two kinds of sheets; one kind consists of $Eu^{2+}$ atoms and the other is a combination of anionic slabs and $Eu^{2+}$ atoms.

In Fig. 1, the sheet of $Eu^{2+}$ atoms marked as C separates two slabs of chains marked as A and B. The individual slabs, A and B are related to each other by *b*-glide symmetry. A single slab is shown, in Fig. 2(a). Each slab in fact consists of chains running along the *c*-axis and the closest distance between two chains is 4.368(3) Å from Sb(8) to Sb(6) as indicated in Fig. 2(b). Eu atoms are nested in the space of anionic chains to form sheet parallel to the *ac*-plane.

A single chain of $[Ga_6Sb_8]^{14-}$ is shown in Fig. 3. It contains homoatomic tetramers $(Ga_4)^{6+}$ and dimers $(Ga_2)^{4+}$ that are connected by sharing Sb atoms to form a "$Ga_6Sb_7$" cluster and the clusters are then bridged by Sb(6) atoms to form the infinite chain $[Ga_6Sb_7Sb_{2/2}]^{14-}$. As the chains organize into a slab "$Ga_6Sb_7$" clusters adopt a close-packed hexagonal arrangement. There are six crystallographically different Ga atoms and eight Sb atoms. The covalent Ga–Ga bonds found range from 2.567(3) to 2.678(3) Å (Table 3). In the tetramer $(Ga_4)^{6+}$, the distances between Ga(1)–Ga(2), Ga(2)–Ga(4), and Ga(4)–Ga(5) are 2.576(3) Å, 2.678(3) Å, and 2.567(3) Å, respectively. In the dimer $(Ga_2)^{4+}$, the distance of Ga(3)–Ga(6) is 2.577(3) Å. These bond lengths are comparable to the sum of covalent Ga radii (2.52 Å) and also comparable to the 2.565(2) Å in $BaGa_2Sb_2$ [5], 2.605(3) Å in $NdGaSb_2$ [17], and 2.586(4) Å in $Pr_{12}Ga_4Sb_{23}$ [8]. The closest distances between the tetramer and the dimer are 2.856(3) and 2.889(3) Å at Ga(2)–Ga(3) and Ga(3)–Ga(4), respectively, which are somewhat long to be considered as single covalent bonds but partial bonding interactions cannot be ruled out.

To our knowledge, gallium phases with homonuclear Ga tetramers and dimers together as in $[Ga_6Sb_8]^{14-}$ unit are unprecedented. The most common building blocks in ternary gallium antimonides are tetrahedra $GaSb_4$ unit and trigonal $GaSb_3$ unit as found in $KGaSb_2$ [18], $KGaSb_4$ [19], $K_2GaSb_2$ [20], $Cs_2GaSb_2$ [21], and $Na_2Ga_3Sb_3$ [22].

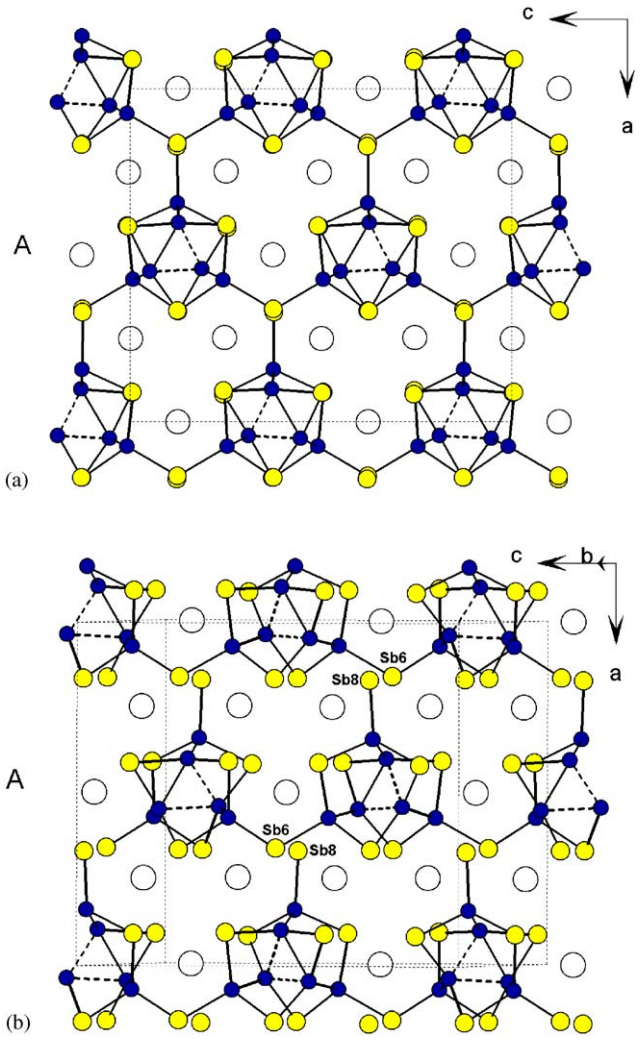


Fig. 2. (a) A [010] view of the first row of chains indicated as A in Fig. 1. The hexagonal packing arrangement of the $[Ga_6Sb_8]^{14-}$ cluster is evident in this view. Due to atomic overlap of eclipsed atoms Sb(6) and Sb(8) in the projection the chains give the appearance of an extended layer. (b) A different view of the slab tilted to show the presence of chains. The closest distance between two neighboring chains is 4.368(3) Å from Sb(6) to Sb(8). The Sb, Ga, and Eu atoms are indicated yellow, blue, and empty circles, respectively.

The Ga atoms are coordinated by different combinations of Sb and Ga atoms. Ga(1), Ga(5), and Ga(6) are coordinated by three Sb atoms and one Ga atom with Ga–Sb bond distances ranging from 2.659(3) to 2.805(2) Å and Ga–Ga distances from 2.567(3) to 2.577(3) Å. The Ga(3) atom is coordinated by two Sb atoms at 2.734(2) and 2.737(3) Å and one Ga atom at 2.577(3) Å, whereas two more Ga atoms lie at 2.856(3) and 2.889(3) Å. Ga(2) atom is coordinated by two Sb atoms at 2.764(3) and 2.698(3) Å and two Ga atoms at 2.576(3) and 2.678(3) Å, where an additional Ga atom is at 2.856(3) Å. Ga(4) atom is coordinated by two Sb

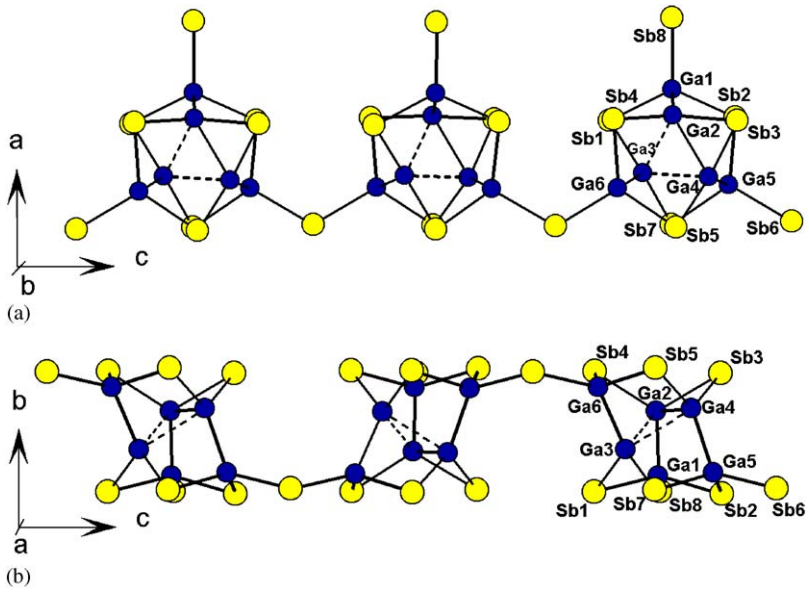


Fig. 3. A single chain of $[Ga_6Sb_8]^{14-}$ viewed down the *b*-axis (a) and view down the *a*-axis (b) showing labels of atoms. The Sb atoms are shown as yellow and the Ga atoms are blue circles.

atoms at 2.683(3) and 2.727(3) Å and two Ga atoms at 2.567(3) and 2.678(3) Å, where an additional Ga atom is at 2.889(3) Å. Therefore, all Ga–Sb bond distances in this compound are in a range of 2.659(3)–2.805(2) Å and they are comparable to those found in previously reported $BaGa_2Sb_2$ [6] and $NdGaSb_2$ [16]. There are no Sb–Sb bonding in the structure. The geometry around Ga atoms is very distorted from commonly known $GaSb_4$ tetrahedra and $GaSb_3$ trigonal planar units. For example, the tetrahedral angles around Ga(6) atom are in a range of 91.94(8)–127.10(10)°. Therefore, the local geometry around the Ga centers is very flexible and adjusts to bonding requirements in order to complete their octet and the size of large cations around.

There are seven crystallographically different Eu atoms $Eu_7Ga_6Sb_8$ (Fig. 4). Eu(1), Eu(6) and Eu(7) atoms are positioned within the sheet (A and B parts in Fig. 1) and have trigonal prismatic geometries. The remaining $Eu^{2+}$ atoms are positioned between the sheets of $[Ga_6Sb_8]^{14-}$ chains (C part in Fig. 1) and have distorted octahedral geometries. The single bond distances of Eu–Sb and Eu–Ga calculated from metallic radii are 3.475 and 3.330 Å, respectively [23]. The distances observed in $Eu_7Ga_6Sb_8$ are comparable to those found in $Eu_5In_2Sb_6$ [4(b)], $Eu_{16}Sb_{11}$ [24], and $Eu_6Ga_2P_6$ [25]. Assuming the formal oxidation state of the tetrameric unit as $(Ga_4)^{6+}$ and the dimer as $(Ga_2)^{4+}$, and all Sb atoms as $Sb^{3-}$, a charged-balanced formula is best represented as $7Eu^{2+}$ $[(Ga_4)^{6+}(Ga_2)^{4+}(Sb^{3-})_8]^{14-}$.

### 3.2. Electronic structure

To better appreciate the chemical bonding in this unusual material, band structure calculations were performed on the anionic $[Ga_6Sb_8]^{14-}$ framework. The band structure was calculated using the extended-Hückel formalism as described previously [5]. In the calculation complete electron transfer from $Eu^{2+}$ atom to anionic framework is assumed to take place. Therefore, we only considered $Eu^{2+}$ atoms as charge balancing "spectator" cations as in other alkali or alkaline earth metal Zintl phases. The agreement between the experimental observation of a 0.6 eV band-gap and the prediction of a band-gap by the calculations confirms that this assumption is correct Fig. 4.

DOS and COOP are shown in Fig. 5. The calculations show that the valence states are completely filled and the Fermi level occur just below the energy gap, which suggests the compound to be a semiconductor. Due to the weakness of this calculation method, the quantitative comparison of the band-gap with the experimentally observed value is not possible. The DOS plot in Fig. 5(a) contains total densities together with projections for the Ga *p* and Sb *p* orbital contributions. The width of the valence band is very narrow located at about −7.5 eV indicating the anionic framework has one-dimensional character. The projected DOS shows that the states near the Fermi level, $E_f$, have mainly contributions from Ga 4*p* and Sb 5*p* orbitals mixed with some corresponding *s* orbital character. The block of states at lower energy (<−10.3 eV) are dominated by *p* orbitals of Sb and the states above −10.3 eV are dominated by *p* orbitals of Ga. This difference in energy derives from their electronegativity difference. According to the Zintl concept, the formal charge of two-bonded Sb atoms can be assigned as $Sb^{1-}$ and that of one-bonded Sb(8) atoms can be assigned as $Sb^{2-}$. However, electron

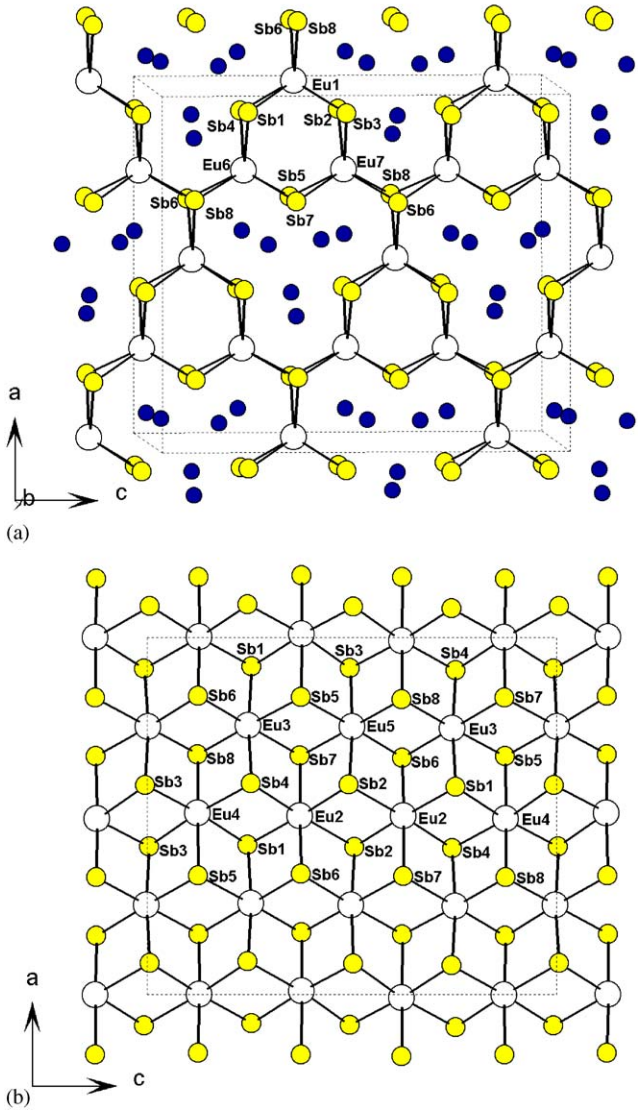


Fig. 4. (a) Local coordination of Eu(1), Eu(6), and Eu(7) atoms (b) Local coordination of Eu(2), Eu(3), Eu(4) and Eu(5) atoms. The Sb, Ga, and Eu atoms are indicated yellow, blue, and empty circles, respectively.

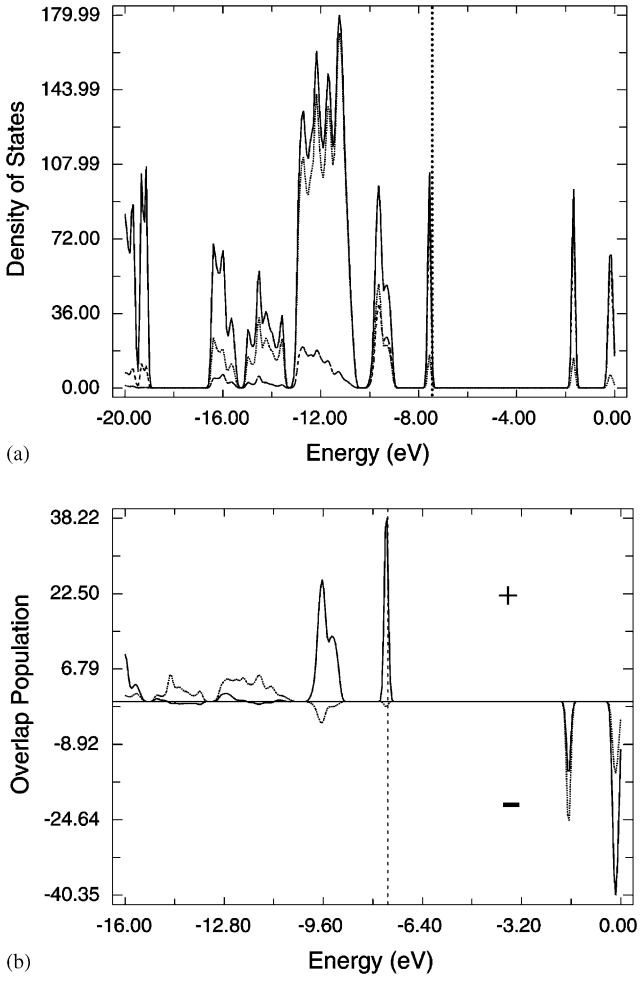


Fig. 5. COOP and DOS curves for $Eu_7Ga_6Sb_8$. (a) Total DOS and projected DOS curves. The projection of Ga 4*p* (dashed line), Sb 5*p* (dotted line), and total DOS (solid line) curves are shown. (b) COOP curves of Ga–Ga (solid line) and Ga–Sb (dotted line) interaction indicate that structure is stabilized by covalent Ga–Ga interactions. The straight dotted line are Fermi levels ($E_f$) in DOS plot and COOP curves.

counting around the Ga atoms is more complex. If we ignore the weak interactions of Ga(3)–Ga(4) interaction at 2.889(3) Å and Ga(3)–Ga(2) at 2.856(3) Å, the compound can be described as two-electron deficient and described as $7Eu^{2+}[(4bGa^{1-})_5(3bGa^{2-})(2bSb^{1-})_7(1bSb)^{2-}]^{16-}$. However, if we count the weak Ga–Ga interactions in the range of 2.856(3)–2.889(3) Å as half bonds, it can be described as a valence precise compound $7Eu^{2+}[(4.5bGa^{0.5-})_2(4bGa^{1-})_4(2bSb^{1-})_7(1bSb)^{2-}]^{14-}$. The band structure calculations support the second description as more reasonable and indicate that the compound electronically is a Zintl phase.

In COOP plots, the projections for Ga–Ga and Ga–Sb bonds are shown in Fig. 5(b). Considering the lower oxidation state of Ga due to homonuclear Ga–Ga bonds, a slight antibonding character is anticipated on the Ga–Sb bonds. However, the states just below $E_f$ are mainly from Ga–Ga bonding interactions that suggests the strong covalent Ga–Ga bonding is predominantly contributing to the stability of the compounds. Some of Ga–Sb antibonding states just below Fermi level are also filled suggesting some weakening of bonding interactions in Ga–Sb.

### 3.3. Magnetic properties

Magnetic susceptibility measurements indicate that Ga/Sb framework is diamagnetic as predicted by the band calculation. The compound's paramagnetism comes exclusively from the magnetic $Eu^{2+}$ ions.

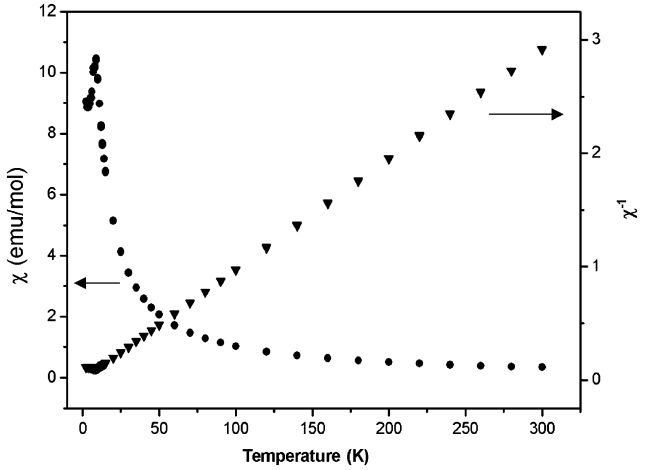


Fig. 6. Magnetic susceptibility and reciprocal susceptibility versus temperature for $Eu_7Ga_6Sb_8$. The circles represent magnetic susceptibility and triangles represent the reciprocal susceptibility.

Magnetic susceptibility measurements indicate that $Eu_7Ga_6Sb_8$ exhibits Curie–Weiss paramagnetic behavior above 9 K, as shown in Fig. 6. The effective magnetic moments calculated from the slope of the $\chi_m^{-1}$ vs. $T$ data is 20.39 $\mu_B$ per formula unit (7.71 $\mu_B$/Eu), which is in good agreement for $Eu^{2+}$ cations ($\mu_{calc} = 7.94\,\mu_B$). This compound orders antiferromagnetically below 9 K. Similar antiferromagnetic transitions at similar temperature have been reported in other Eu compounds such as $Eu_{16}Sb_{11}$ and $Eu_{14}InPn_{11}$ ($Pn$ = Sb, Bi) [24,26].

## Acknowledgments

Financial supports from Korea Research Foundation (KRF-2003-042-C00065) and the Center for Fundamental Materials Research are gratefully acknowledged. Financial support from the Department of Energy (Grant # DE-FG02-99ER45793 to MGK) is gratefully acknowledged. This work made use of the SEM/EDS facilities of the Center of Advanced Microscopy at Michigan State University.

**Supporting information**. Further details of the crystal structure investigation can be obtained from the Fachinformationszentrum Karlsruhe, 76344 Eggenstein-Leopoldshafen, Germany (fax: (49) 7247-808-666; e-mail: crysdata@fiz.karlsruhe.de). The depository number for $Eu_7Ga_6Sb_8$ compound is CSD 413737.

## References

[1] S.M. Kauzlarich (Ed.), Chemistry, Structure, and Bonding of Zintl Phases and Ions, VCH Publishers, Inc, New York, 1996.
[2] S.-J. Kim, J. Slavador, D. Bilc, S.D. Mahanti, M.G. Kanatzidis, J. Am. Chem. Soc. 123 (2001) 12704.
[3] S.-J. Kim, S. Hu, C. Uher, M.G. Kanatzidis, Chem. Mater. 11 (1999) 3154.
[4] (a) S.-J. Kim, J. Ireland, C.R. Kannewurf, M.G. Kanatzidis, J. Solid State Chem. 155 (2000) 55;
(b) S.-M. Park, E.-S. Choi, W. Kang, S.-J. Kim, J. Mater. Chem. 12 (2002) 1839.
[5] S.-J. Kim, M.G. Kanatzidis, Inorg. Chem. 40 (2001) 3781.
[6] S.-M. Park, S.-J. Kim, M.G. Kanatzidis, J. Solid State Chem. 175 (2003) 310.
[7] (a) G. Cordier, H. Schäfer, M. Stelter, Z. Anorg. Allg. Chem. 519 (1984) 183;
(b) S.L. Brock, L.J. Weston, M.M. Olmstead, S.M. Kauzlarich, J. Solid State Chem. 107 (1993) 513;
(c) S.M. Kauzlarich, M.M. Thomas, D.A. Odink, M.M. Olmstead, J. Am. Chem. Soc. 113 (1991) 7205;
(d) S.M. Kauzlarich, T.Y. Kuromoto, Croat. Chim. Acta 64 (1991) 343;
(e) D.M. Young, C.C. Torardi, M.M. Olmstead, S.M. Kauzlarich, Chem. Mater. 7 (1995) 93.
[8] A.M. Mills, A. Mar, Inorg. Chem. 39 (2000) 4599.
[9] J.I. Pankove, Optical Process in Semiconductors, Dover Publication, New York, 1976.
[10] (a) J.W. Lyding, H.O. Marcy, T.J. Marks, C.R. Kannewurf, IEEE Trans. Instrum. Meas. 37 (1988) 76;
(b) H.O. Marcy, T.J. Marks, C.R. Kannewurf, IEEE Trans. Instrum. Meas. 39 (1990) 756.
[11] (a) R. Hoffman, J. Chem. Phys. 39 (1963) 1397;
(b) E. Canadell, M.-H. Whangbo, Chem. Rev. 91 (1991) 965.
[12] (a) M. Wolfsberg, L. Helmholz, J. Chem. Phys. 20 (1952) 837;
(b) C.J. Ballhausen, H.B. Gray, Molecular Orbital Theory, Benjamin, New York, 1965;
(c) H. Basch, A. Viste, H. Gray, Theor. Chim. Acta 3 (1965) 458;
(d) H. Basch, A. Viste, H. Gray, J. Chem. Phys. 44 (1966) 10;
(e) V. Baranovskii, A. Nikolskii, Theor. Eskp. Khim. 3 (1967) 527.
[13] J. Ren, W. Liang, M.-H. Whangbo, CAESAR 1.0 Primecolor Software, Inc. Cary, North Carolina, 1998.
[14] SMART and SAINT Version 5: Siemens Analytical X-ray System, Inc., Madison, WI, 1998.
[15] G.M. Sheldrick, SADABS, University of Gottingen, Göttingen, Germany.
[16] G.M. Sheldrick, SHELXS-97 and SHELXS-97, University of Göttingen: Göttingen, Germany, 1997.
[17] A.M. Mills, A. Mar, J. Am. Chem. Soc. 123 (2001) 1151.
[18] G. Cordier, H. Ochmann, Z. Kristallogr. 195 (1991) 297.
[19] G. Cordier, H. Ochmann, Z. Kristallogr. 195 (1991) 306.
[20] (a) G. Cordier, H. Ochmann, H. Schäfer, J. Less-Common Met. 119 (1991) 291;
(b) G. Cordier, H. Ochmann, Z. Kristallogr. 195 (1991) 115.
[21] G. Cordier, H. Ochmann, Z. Kristallogr. 195 (1991) 310.
[22] G. Cordier, H. Ochmann, H. Schäfer, Mater. Res. Bull. 21 (1986) 331.
[23] L. Pauling, The Nature of the Chemical Bond, Cornell Press, Ithaca, NY, 1960, p. 403.
[24] J.Y. Chan, M.M. Olmstead, H. Hope, S.M. Kauzlarich, J. Solid State Chem. 155 (2000) 168.
[25] M. Somer, W. Carrillo-Cabrera, K. Peters, H.G. von Schnering, G. Cordier, Z. Kristallogr. 211 (1996) 257.
[26] J.Y. Chan, M.E. Wang, A. Rehr, S.M. Kauzlarich, D.J. Webb, Chem. Mater. 9 (1997) 2131.